Reversible Pinocytosis in Polymorphonuclear Leukocytes

GAIL DAUKAS, DOUGLAS A. LAUFFENBURGER, and SALLY ZIGMOND
Biology Department and Chemical Engineering Department, University of Pennsylvania, Philadelphia, Pennsylvania 19104

ABSTRACT Since pinocytosis has only been recently recognized in polymorphonuclear leukocytes (PMNs), little is known about the fate of pinosomes. Here we report that pinosomes can fuse with the cytoplasmic granules of PMNs. We also find that at least for a short period of time after formation, pinosomes can fuse with the plasma membrane and release their contents to the outside. We present a morphological description and biochemical data on the kinetic parameters of a steady state pool of reversible pinosomes in PMNs.

In addition, we have developed conditions under which pinosomes continue to form and fuse with the plasma membrane but fail to fuse with the cytoplasmic granules, i.e., only "reversible" pinocytosis occurs. This inhibition of fusion with the granules is not due to an inability of the pinosomes to move from the surface since under these conditions pinosomes labeled with an electron-dense marker can be seen in the cell interior.

Recent studies have demonstrated that there are multiple fates for pinosomes. In most cells, the content of pinosomes is delivered to lysosomes. However, this is not always the case and some materials taken up into pinosomes are transported to the Golgi apparatus or entirely across the cell (1, 11). Even when the endocytosed proteins do eventually go to lysosomes, they may move first to an intermediate, prelysosomal compartment (22, 32). In situations where the pinosome content is deposited in an intracellular compartment, the pinosome membrane appears to recycle back to the plasma membrane (3, 19, 25, 33). Though the recycling is presumed to be vesicular, there is little evidence to support this.

One possible consequence of a vesicular mechanism of membrane retrival from intracellular compartments is that some of the material in those compartments will be passively carried out and released from the cell. Indeed, several recent reports have shown that some of the material taken up by pinocytosis is subsequently released into the medium (2, 5, 30, 31).

In this report we show that in polymorphonuclear leukocytes (PMNs) some of the material taken up via pinocytosis is rapidly returned to the medium intact. We demonstrate that this release results from pinosomes fusing with the plasma membrane and emptying their contents to the outside. We refer to this pathway as reversible pinocytosis. In addition, we show that while pinosomes normally fuse with the electron-dense granules of PMNs, this fusion can be blocked by metabolic inhibitors and hypertonic sucrose. This inhibitor cocktail does not block the formation of pinosomes, or the fusion between the pinosome and the plasma membrane, i.e., it does not interfere with the reversible pinocytosis pathway. Finally, we show that the inhibition of fusion between pinosomes and granules is not due to immobilization of the pinosomes near the surface, since labeled pinosomes are found in the interior of the cell.

MATERIALS AND METHODS

Cells: Rabbit peritoneal exudate cells are collected 4 h after injection of 0.1 g of shellfish glycogen (Schwartz/Mann Div., Becton-Dickinson & Co., Orangeburg, NY) in 250 ml of 0.9% saline. Contaminating erythrocytes, if present, are lysed by brief (60 s) treatment with hypotonic (0.18%) saline. The cells are washed twice with 0.9% saline and resuspended in Hank's balanced salt solution (HBSS) (Grand Island Biological Co., Grand Island, NY) buffered with 2.4 mg/ml of HEPES (Sigma Chemical Co, St. Louis, MO) at a concentration of 3.3×10^6 cells/ml. 3 ml of the cell suspension is placed in 60 × 15 mm petri dishes (Falcon Labware, Div. of Becton-Dickinson & Co., Oxnard, CA) and the cells are allowed to settle for 15 min at 23°C. Dishes are checked with an inverted microscope (Olympus Corporation of America, New Hyde Park, NY) to ensure that the an even monolayer has formed.

Peptide Uptake and Release: Cells are incubated for various times with [^{3}H]*N*-formylnorleucylleucylphenylalanine (FNLLP) at 37°C and then washed for >5 min at 4°C. A 5-min wash has been shown to remove >86% of the receptor-bound peptide (29). The peptide (counts per minute [CPM]) remaining cell-associated after this wash is the "total uptake." To measure release of the cell-associated radioactivity, cells incubated in [^{3}H]-FNLLP and then washed are returned to 37°C in HBSS. After various times at 37°C, the medium is removed, and the tritium released into the medium and that remaining with the cells is counted. In some experiments, cells were incubated in an "inhibitor cocktail" consisting of glucose-free HBSS containing 5 mM 2-deoxy-D-glucose (Sigma Chemical Co.), 1 mM sodium fluoride (Sigma Chemical Co.), and 0.3 M sucrose at 37°C for 30 min prior to the beginning of the experiment and during the period when uptake and/or release were measured.

Peptide Digestion: Peptide digestion is assayed by partitioning into ethyl acetate and/or by thin layer chromatography (TLC). For partitioning, the aqueous medium containing the peptide is brought to pH 2 with 1 N HCl, and an equal volume of ethyl acetate is added. After thorough mixing, the solution is

THE JOURNAL OF CELL BIOLOGY · VOLUME 96 JUNE 1983 1642-1650

allowed to separate into two phases. The intact FNLLP, having a blocked amino group, partitions into the ethyl acetate, while any digestion products having a free amino group (which is protonated at pH 2) will remain in the aqueous phase. The peptide is labeled with [^{3}H]phenylalanine. Thus we detect the removal of the formyl group or the cleavage of either peptide bond by counting the radioactivity in the aqueous phase.

For TLC analysis, an aliquot of the medium is spotted onto a precoated silica gel 60 F_{254} TLC sheet (EM Reagents, Darmstadt, Federal Republic of Germany). The TLC is run in a chloroform:methanol:acetic acid:water (60:30:4:1) solvent. It is then cut into one-quarter inch strips which are counted. The ratio to the solvent front of the intact peptide is 0.7 and that of the Phe peak (the major product) is 0.2.

Electron Microscopy: Cells are processed for electron microscopy by the method of Bainton and Farquhar (4). Briefly the cells are fixed in 2.5% gluteraldehyde, postfixed in 1% osmium tetroxide, stained en bloc with uranyl acetate, dehydrated and embedded according to the method of Spurr (27). The presence of peroxidase was detected cytochemically using the diaminobenzidine method of Graham and Karnovsky (13). Sections were examined without lead citrate staining, using a JEOL 100S transmission electron microscope at 60 kV.

For quantitative analysis of EM specimens random samples were obtained following the method of Steinman et al. (28). Several different areas from each cell pellet were sectioned and analyzed. We took care to ensure that only sections with silver interference colors were used. We examined every cell profile in a section at final magnification 25,000. The number of colloidal gold particles per profile were counted and expressed as a function of the cytoplasmic area. In addition, randomly selected cell profiles were examined for the presence of colloidal gold in cytoplasmic granules. We determined cytoplasmic area by morphometric analysis using a microprocessor linked digital planimeter (23, 24).

Preparation of Colloidal Gold: Colloidal gold coated with bovine serum albumin (BSA) (fatty-acid-free) (Sigma Chemical Co.) was prepared by the method of Horisberger and Rosset (15) and Geoghegan and Ackerman (12). Briefly, 20 mg of gold chloride (ICN Pharmaceuticals, Inc., Cleveland, OH) in 200 ml of distilled water was brought to a boil. 6 ml of 1% sodium citrate was added and the solution boiled until it became orange-reddish. The solution was allowed to cool to room temperature and 23 ml of 1 mg/ml solution of BSA was added and mixed for 2 min. 1% polyethylene glycol (20,000 mol wt) was then added to prevent aggregation. The conjugated gold was spun at 15,000 rpm for 1 h, the pellet was resuspended in HBSS or glucose-free HBSS plus 5 mM 2-deoxy-D-glucose, 1 mM sodium fluoride, and 0.3 M sucrose.

Iodination of BSA: BSA (fatty-acid-free) was labeled with Na ^{125}I (Amersham Corp., Arlington Heights, IL; 100 mCi/ml, carrier-free) by the chloroamine-T method (16). BSA degradation was monitored by precipitation with 10% trichloroacetic acid. Radioactivity was measured in a LKB 1270 Rackgamma counter (LKB Instruments, Inc., Gaithersburg, MD).

RESULTS

Reversible Pinocytosis

Previously we have shown (29) that rabbit peritoneal PMNs accumulate the chemotactic peptide, FNLLP via both receptor-mediated and bulk-fluid pinocytosis. The internalized peptide is partitioned into at least two pools; the peptide from one pool gets digested and is released into the medium, while the peptide in the other pool is stored in the cell for at least 6 h (35).

We have now more thoroughly investigated the intracellular processing of exogenous material and have evidence for a third fate for internalized material. Our data is consistent with the model seen in Fig. 1. We propose that in PMNs a newly formed pinosome can fuse with the plasma membrane emptying its content to the outside or it can fuse with intracellular compartments where its contents will either be digested or stored.

When cells that have taken up ^{3}H-FNLLP at 37°C are washed 5 min at 4°C and returned to 37°C, they release radioactive counts into the medium (Fig. 2). The radioactivity released consists of both digested (primarily phenylalanine) and intact peptide. The amount of intact peptide released is temperature dependent with little release occurring at 0°C. Over the same period, the release at 0°C is <20% of the release at 37°C when uptake is done in 2×10^{-8} M ^{3}H-FNLLP. Furthermore, cells can be incubated up to 60 min at 4°C (when 100% of the surface receptor-bound peptide has been removed

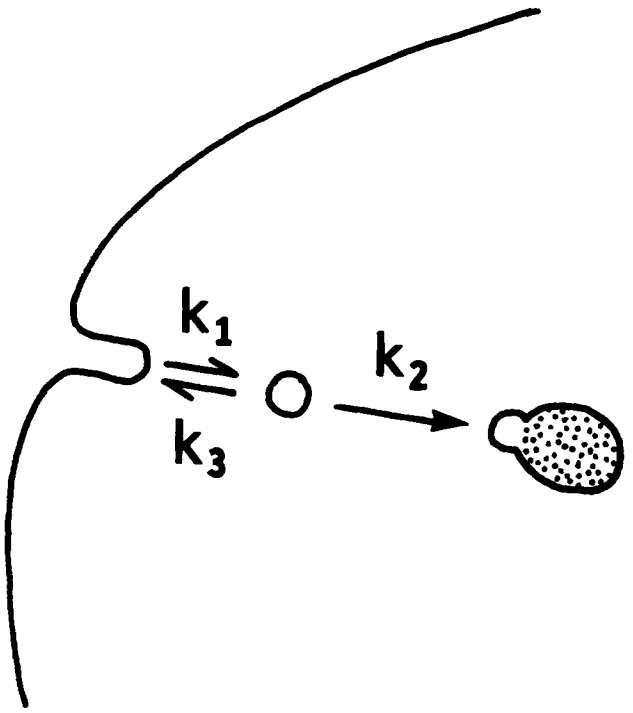

FIGURE 1 Model of pathways of pinosome movement. The kinetics of pinosome movement are described by three rate constants: (*i*) the formation of pinosomes is described by k_1, the rate constant of endocytosis; (*ii*) the exocytosis of pinosomes is described by k_3, the rate constant of release of intact material from cells; (*iii*) the further processing of pinosomes by the cell is described by k_2, the rate constant of either digestion or storage of internalized material.

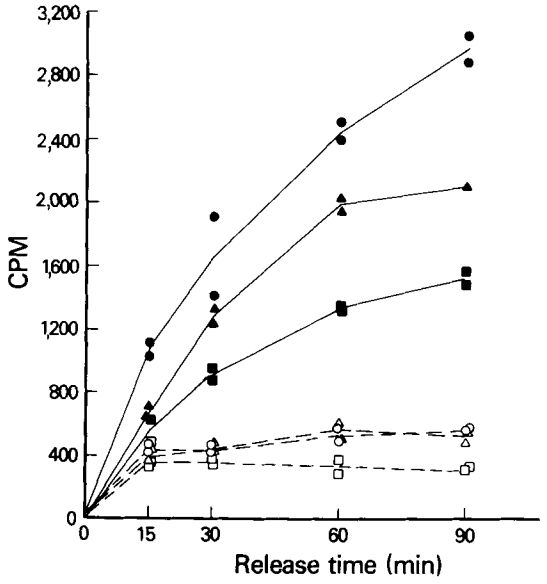

FIGURE 2 Time course of peptide release. PMNs are incubated with 2×10^{-8} M ^{3}H-FNLLP at 37°C for 15 (■, □), 30 (▲, △), or 75 (●, ○) min. The cells are washed for 5 min at 4°C and then incubated with fresh HBSS for different periods of time at 37°C. The medium is then removed and analyzed. Radioactivity is separated into a digested fraction and intact peptide by partitioning into ethyl acetate from an aqueous phase at pH 2. (—) Digested peptide. (- - -) Intact peptide.

[29]) and the subsequent release at 37°C is uneffected. As can be seen in Fig. 2, the release of intact peptide is rapid and transient while the release of digested peptide continues over

the 90 min studied. It has previously been shown that amino acids and some dipeptides can diffuse across lysosomal and plasma membranes. However, larger molecules remain trapped within lysosomes (10, 18). Thus the release of intact peptide into the medium was unexpected.

To determine the source of the released intact peptide, we first ruled out the possibility that surface receptor-bound peptide could account for this release. If the source of intact peptide release were receptor-bound peptide then the amount released should plateau as receptors become saturated with increasing concentrations of peptide. In contrast, as shown in Fig. 3, the amount of intact peptide released is proportional to the amount of peptide taken up by the cells even in peptide concentrations (i.e., 2×10^{-5} M) 100 times that which saturates all the surface receptors (29). In fact, the amount of intact peptide released after incubations in high concentrations of peptide exceeds the number of surface receptors by 1,000-fold.

If the intact peptide is released through pinosomes fusing with the plasma membrane, we should see a similar release of other pinocytic markers, such as ^{125}I-BSA. To test for this, cells were incubated for 30 min at 37°C with ^{125}I-BSA plus 2×10^{-8} M unlabeled FNLLP (to stimulate pinocytosis) and then washed extensively at 4°C. The release of TCA-precipitable BSA was followed for various periods of time at both 4°C and 37°C. TCA-precipitable BSA is released at 37°C but not at 4°C. The kinetics of the release are similar to that of intact peptide release (Fig. 4). The percentage of total cell-associated material (peptide or BSA) that is released intact into the medium depends upon the duration of the uptake phase of the experiment and continually declines with periods of uptake >15 min. Under the conditions examined, ~10% of the material (peptide or BSA) accumulated during a 30-min uptake is released intact (Figs. 3 and 4). The accumulation and intracellular fate of BSA has also been followed using colloidal gold particles coated with BSA (BSA-gold). Morphological studies presented later in the paper provide direct evidence that BSA-gold is found within intracellular vesicles and is subsequently released from the cells with a time course similar to that for the release of intact ^{125}I-BSA.

Finally, to rule out the possibility that this release is due to fluid trapped between the cells and the dish and thus inaccessible to washes at 4°C, we repeated both the peptide and BSA experiments using cells in suspension. The results are identical to those using plated cells. Thus, all of the evidence is consistent with the hypothesis that the release of intact peptide is due to the exocytosis of internalized peptide.

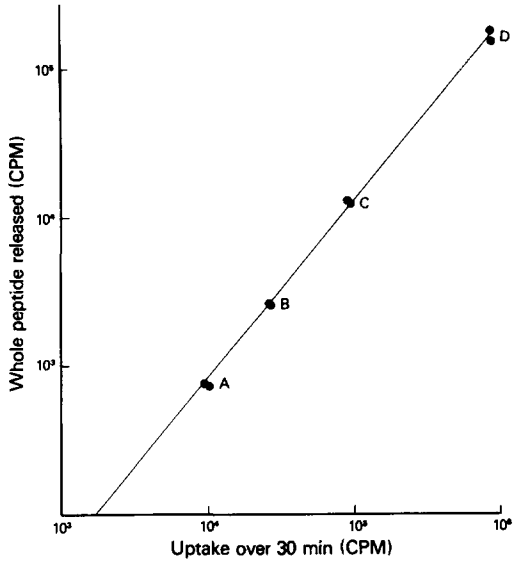

FIGURE 3 Dose response of intact (whole) peptide release. PMNs are incubated with various concentrations of ^{3}H-FNLLP at 37°C for 30 min, washed, and incubated at 37°C for 30 min. The peptide taken up and the intact peptide released are plotted for each concentration. ($A = 2 \times 10^{-8}$ M, $B = 2 \times 10^{-7}$ M, $C = 2 \times 10^{-6}$ M, $D = 2 \times 10^{-5}$ M).

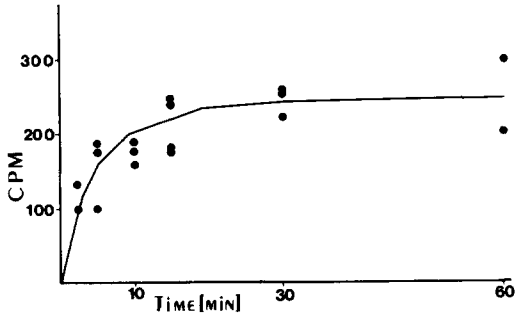

FIGURE 4 Time course of release of TCA-precipitable BSA. PMNs are incubated with 2×10^{-8} M unlabeled FNLLP, ^{125}I-BSA (6.5 μCi/ml) and 1% unlabeled BSA at 37°C for 30 min, and then are washed for 10 min at 4°C. At this point, there were 2,128 cpms remaining cell associated. The cells are then incubated with fresh HBSS for different periods of time at 37°C. The medium is removed and analyzed for the presence of TCA-precipitable counts. The release at 4°C over a 30-min period was ~20% of that released at 37°C.

Inhibition of Pinosome—Granule Fusion

Incubation of cells in a cocktail of inhibitors (5 mM 2-deoxy-D-glucose, 1 mM sodium fluoride and 0.3 M sucrose in HBSS

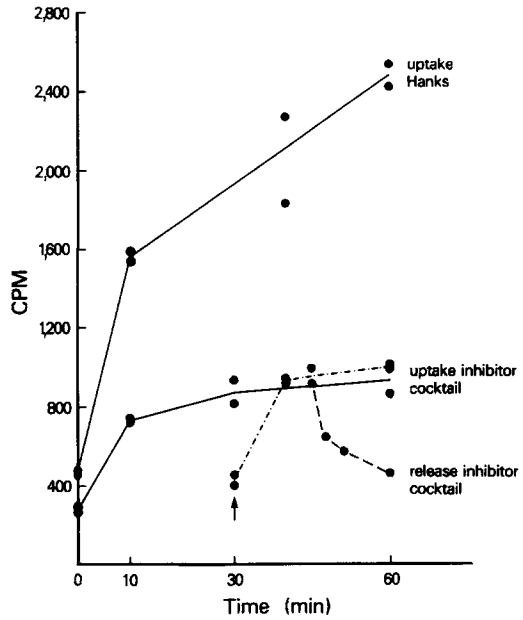

FIGURE 5 Effect of inhibitor cocktail on peptide uptake and release. The uptake of ^{3}H-FNLLP (2×10^{-8} M) was followed in control cells and in cells pretreated and tested in the inhibitor cocktail (5 mM 2-deoxy-D-glucose, 1 mM sodium fluoride, and 0.3 M sucrose) (—). Background counts were the counts seen after a 5-min exposure of cells to 2×10^{-8} M ^{3}H-FNLLP at 4°C followed by a 5-min wash. To examine the transient nature of the uptake in the inhibitors, we incubated cells in inhibitor cocktail in 2×10^{-8} M unlabeled FNLLP and at 30 min (arrow) the unlabeled FNLLP was removed and 2×10^{-8} M ^{3}H-FNLLP was added and its uptake followed (-·-). At 45 min, cells were removed and washed at 4°C. Release of radioactivity is measured at 37°C in inhibitor cocktail (- - -).

without glucose) inhibits the digestion and long term storage of peptide but does not inhibit the uptake of peptide into a reversible compartment. As can be seen in Fig. 5, FNLLP is taken up by PMNs in this inhibitor cocktail and the amount of peptide accumulated reaches a plateau in ~15 min. This plateau could be due either to an inhibition of pinocytosis after an initial period of uptake or to a steady state in which peptide continues to be taken up but is released at an equal rate. To distinguish between these two possibilities, we pretreated the cells with the inhibitor cocktail and unlabeled FNLLP for 30 min and then exchanged the unlabeled FNLLP for an equal concentration of ^{3}H-FNLLP. As shown in Fig. 5, the same amount of ^{3}H-FNLLP is accumulated whether the ^{3}H-FNLLP is added at time 0 or later in exchange for unlabeled peptide. When the cells were washed free of peptide and then reincubated in the presence of inhibitors, they released all of the accumulated radioactivity as intact peptide. Further examination demonstrates that the kinetics of this release are identical to that seen under normal conditions (i.e., $t_{1/2} = 4$ min or a rate constant of 0.173 min^{-1}) (see below). Thus all the peptide accumulated in the presence of the inhibitors remains in the reversible pool.

Morphological Identification of Reversible Pinosomes

When pinocytosis is stimulated by the addition of 2×10^{-8} M unlabeled FNLLP in the presence of BSA-coated colloidal gold, the gold subsequently appears in both electron-lucent vesicles and electron-dense granules (Fig. 6). It appears that the majority of this uptake is via fluid-phase for there was an insignificant amount of colloidal gold bound to the surface of the cells. In Fig. 6, the cells have been stained for peroxidase activity. Colloidal gold can be seen in granules which are clearly peroxidase-positive as well as in granules with little or no peroxidase activity. In PMNs, there are at least two populations of granules: the azurophil granule which contains myeloperoxidase and the specific granule which is peroxidase-negative (4). However, we, and others (14), have found that after stimulation of PMNs with chemotactic peptides, the morphology of the granules is altered. As a result, it is difficult to unambiguously identify two distinct granule populations. The peroxidase-positive granules are clearly azurophil granules. Although the peroxidase-negative granules are presumably specific granules, a label which uniquely stains the specific granule would be required for definitive identification.

The colloidal gold taken up by cells in the presence of the inhibitor cocktail is found only in electron-lucent vesicles (Fig. 7). It is never seen in densely staining granules. In cells treated with the inhibitors, none of the 18 cell profiles examined had gold in electron-dense granules while under control conditions, 20 out of 30 profiles examined had gold particles in electron-dense granules ($G = 21.78$; $P \leq 0.00001$, G-test of independence with Yates correction). The electron-lucent vesicles formed in the presence of the inhibitor cocktail are heterogeneous in size and are distributed throughout the cytoplasm. The size and distribution of these vesicles is similar to that seen for the vesicles mediating colloidal gold uptake in control cells.

When cells incubated in the inhibitor cocktail plus colloidal gold are returned to the inhibitor cocktail without any gold present, the gold is lost from the cells. As seen in Fig. 8, the number of colloidal gold particles per cell profile is dramatically decreased during a 15-min incubation. There were an average of 14.9 (SEM = 3.0, $n = 19$) colloidal gold particles

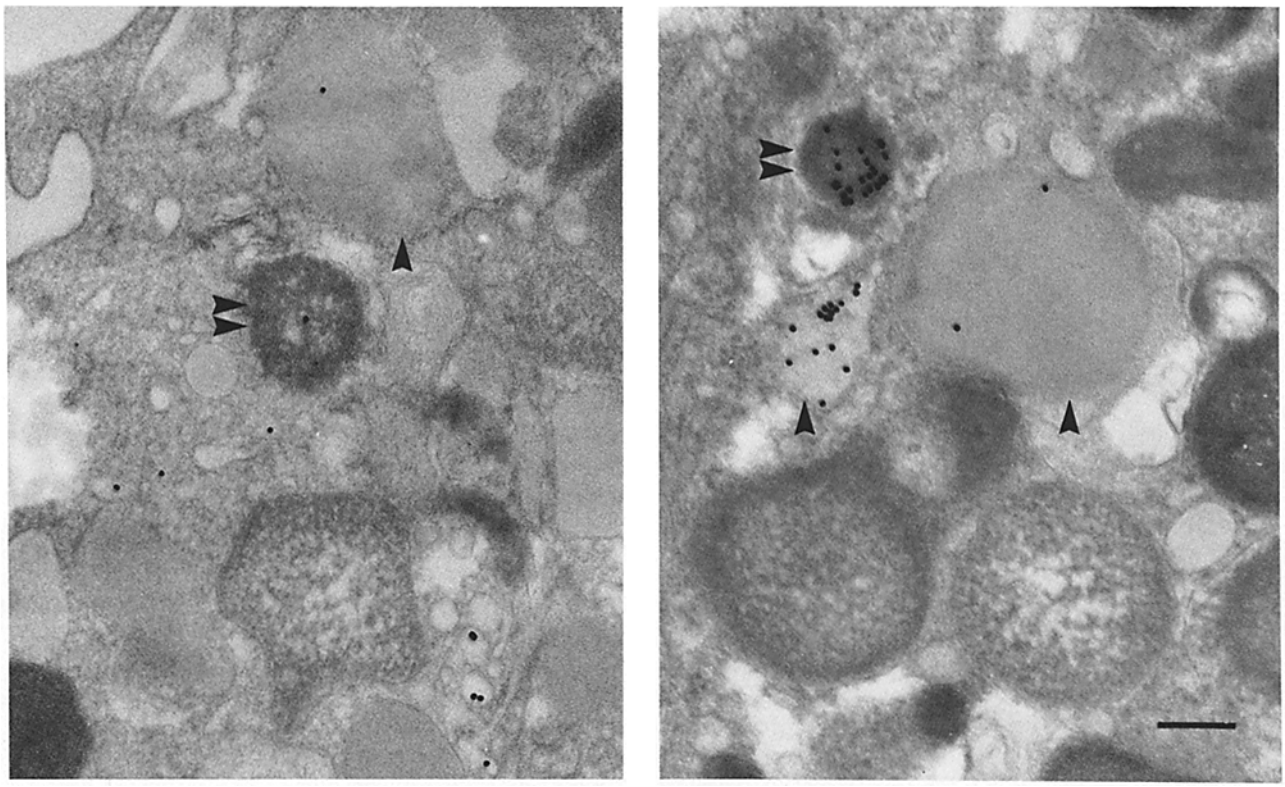

FIGURE 6 Peptide-stimulated colloidal gold internalization. Rabbit PMNs are incubated with 2×10^{-8} M FNLLP and BSA-coated colloidal gold particles at 37°C for 1 h. The cells were processed for EM as described in Materials and Methods. The cells were stained for the presence of peroxidase. Single arrowheads point to peroxidase-negative granules containing BSA-gold. Double arrowheads point to peroxidase-positive granules. Bar, 0.25 μm. × 40,000.

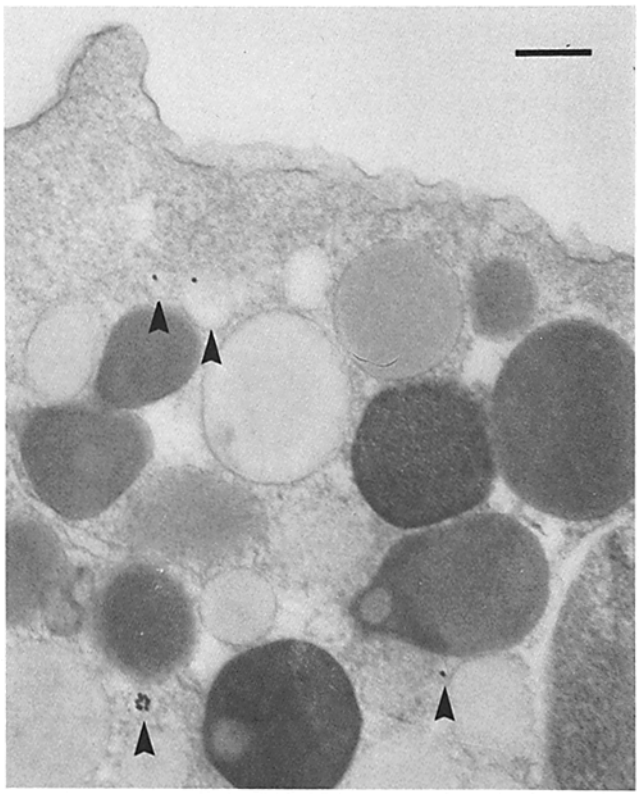

FIGURE 7 Peptide-stimulated colloidal gold internalization in inhibitor cocktail. Rabbit PMNs are incubated with 2×10^{-8} M FNLLP and BSA-coated colloidal gold particles at 37°C for 15 min. The cells were processed for TEM as described in Materials and Methods. Arrowheads point to pinosomes containing BSA-gold. Bar, 0.4 μm. × 25,000.

per 25 μm^2 of cytoplasmic area after the 15-min uptake period and only 2.6 (SEM = 1.3, n = 13) colloidal gold particles per 25 μm^2 of cytoplasmic area after a subsequent 15-min release period in the absence of any gold. When uptake of colloidal gold occurred in the absence of inhibitors, much of the gold remains intracellular following a 15-min release period. There were an average of 19.5 (SEM = 3.0, n = 11) colloidal gold particles per 25 μm^2 of cytoplasmic area after the 15-min uptake period and 10 (SEM = 2.4, n = 18) colloidal gold particles per 25 μm^2 of cytoplasmic area after a subsequent 15-min release period. Thus, in the presence of the inhibitor cocktail, the vesicles labeled with colloidal gold undergo reversible pinocytosis.

Kinetics of Reversible Pinocytosis

The rate of whole peptide release is examined in Fig. 9. PMNs incubated with ^{3}H-FNLLP for 30 min at 37°C were washed and the release of intact peptide was monitored during subsequent incubation at 37°C in HBSS. It can be seen from Fig. 9*a* that intact peptide release is complete within 30 min. A semilogarithmic plot of the release time yields a $t_{1/2}$ = 3.5 min or a rate constant of 0.198 min^{-1} (Fig. 9*b*). This rate constant is the sum of $k_2 + k_3$ (see Eq. 7 in Appendix and Fig. 1). We will refer to it as the rate constant for depletion of material in the reversible pinocytic pool. To determine the time required to fill the compartment which undergoes reversible pinocytosis, we incubated PMNs with ^{3}H-FNLLP for various periods of time and then measured the total amount of intact peptide released during a subsequent 30-min incubation in fresh HBSS (no further release of intact peptide occurred with longer times of incubation) (Fig. 10). A semilogarithmic plot

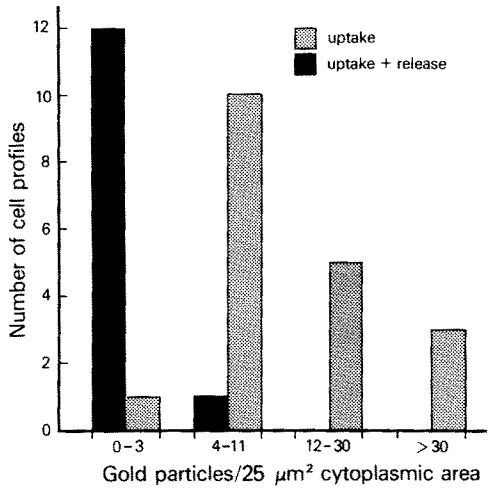

FIGURE 8 Morphometric analysis of reversible pinocytosis. PMNs were incubated with colloidal gold in inhibitor cocktail for 15 min at 37°C (stippled bar). PMNs were incubated as described above, washed free of the gold, and incubated in the inhibitor cocktail for an additional 15 min at 37°C (solid bar).

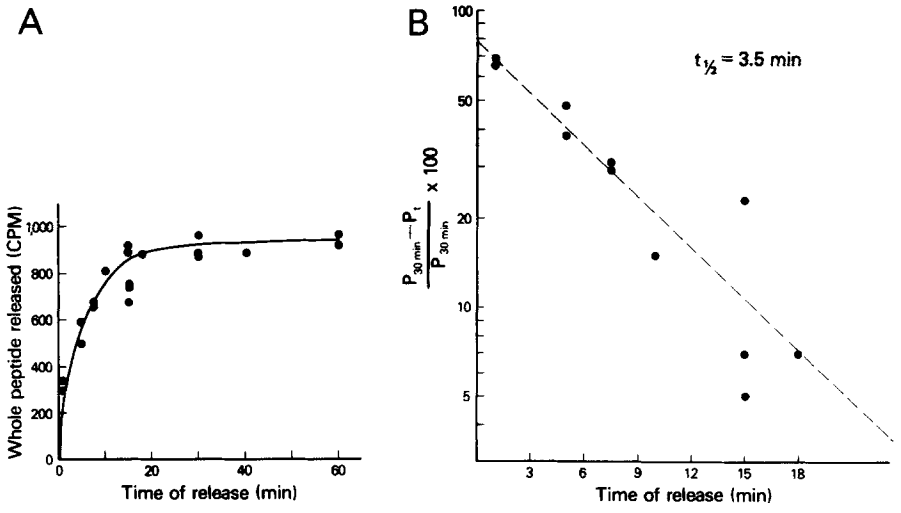

FIGURE 9 Time course of release of intact (whole) peptide. (*A*) PMNs are incubated with 2×10^{-8} M ^{3}H-FNLLP for 30 min, washed, and incubated for different periods of time at 37°C. (*B*) Intact peptide release is plotted semilogarithmically as a function of release time. ($P_{30\,min}$) Amount of intact peptide released by 30 min; (P_t) amount of intact peptide released by time t. The r value for the calculated line is 0.9.

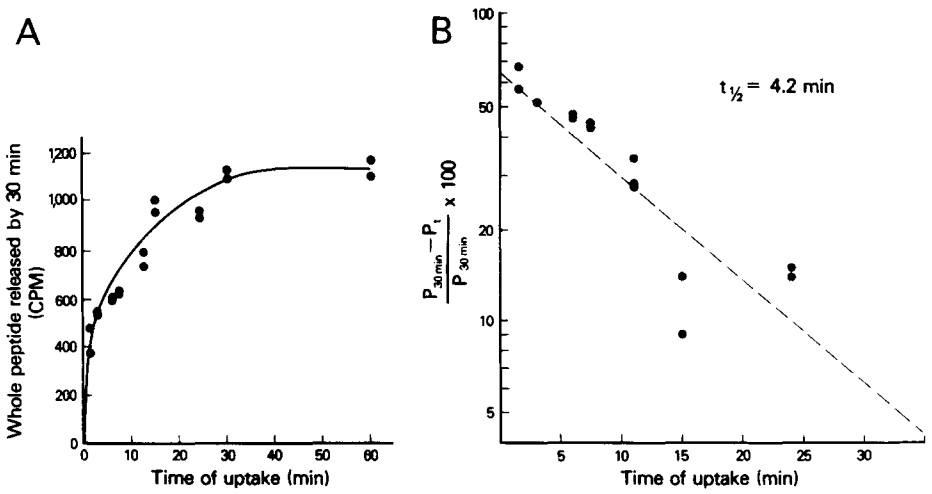

FIGURE 10 Time course of filling the pool of releasable intact (whole) peptide. (*A*) Cells were incubated at 37°C with 2×10^{-8} M ^{3}H-FNLLP for various periods of time, washed, and incubated at 37°C for 30 min. (*B*) Intact peptide release $(P_{30\,min} - P_t)/P_{30\,min}$ is plotted semi-logarithmically as a function of uptake time. ($P_{30\,min}$) Amount of intact peptide released after uptake for times greater than 30 min. (P_t) Amount of intact peptide released within 30 min after uptake for time t. The r value for the calculated line is 0.9.

of the pool content vs. the time of filling yields a $t_{1/2} = 4.2$ min or a rate constant of 0.165 min^{-1}.

As noted in Fig. 2, the release of intact peptide quickly reaches a plateau while the release of digested peptide continues. The cessation of intact peptide release could be due to the fact that no more intact peptide exists in the cell. To examine this possibility, we incubated cells with peptide, then washed them and continued incubation without peptide at 37°C for 2 h. Intact peptide release was complete by 30 min and no further release was seen during the subsequent 1.5-h incubation. We then extracted the remaining cell-associated radioactivity with ethanol recovering >95% of the counts. As can be seen in Fig. 11, the extract is shown to contain both intact and digested peptide when examined by TLC. Therefore the termination of intact peptide release is not due to the depletion of the intact peptide remaining intracellular. Rather, we propose that intact peptide is initially in a compartment which undergoes reversible pinocytosis and later accumulates in another compartment, which does not fuse with the plasma membrane.

The processing of pinocytosed fluid as depicted in the model in Fig. 1 can be described by the following equations. The filling of the reversible pinocytic pool can be described by $dA_p/dt = k_1 M_o - (k_2 + k_3)A_p$, the release of this pool is described by $dA_p/dt = -(k_2 + k_3)A_p$ and $dA_r/dt = k_3 A_p$, and the accumulation of extracellular material through pinocytosis $U = k_2 A_{pss}$, where M_o equals concentration of peptide present outside the cell during uptake (cpm/L); A_p equals the amount of intact peptide in pinocytic pool which can undergo reversible pinocytosis (cpm/cell); A_r equals the amount of intact peptide released (cpm/cell); k_1 equals the rate constant of endocytosis (L/cell/min), k_2 the rate constant of further processing of peptide by the cell (min^{-1}), and k_3 the rate constant of release of intact peptide (min^{-1}); and U equals the total peptide uptake after reversible pinocytic pool, A_{pss}, is at steady state (cpm/cell/min). From these three equations we can derive values for all three rate constants. This derivation is contained in the Appendix. The values obtained are listed in Table I.

One consequence of reversible pinocytosis is that only a portion of the incoming pinosomes or pinosome content will be processed by the cell and contribute to the intracellular accumulation of extracellular markers. The probability that pinocytosed material will be released intact can be estimated from the ratio $k_3/(k_2 + k_3)$, which is approximately 0.5 as seen in Table I. Thus ~50% of the material taken into a cell gets rapidly released. One corollary of this observation is that the

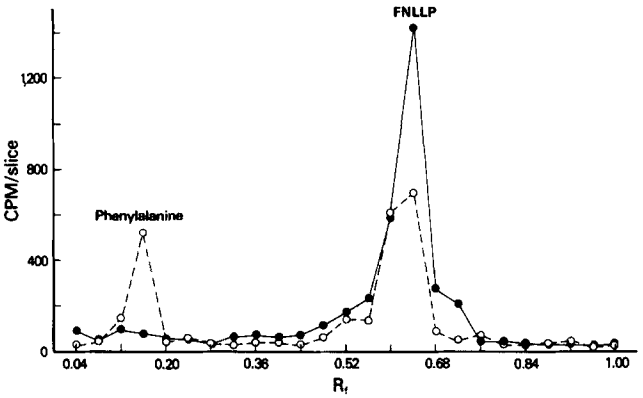

FIGURE 11 Examination of radioactivity remaining cell-associated after intact peptide release is complete. Cells are incubated with ^{3}H-FNLLP for 1 h, washed at 4°C, then incubated for 2 h at 37°C. Greater than 95% of the counts remaining in the cell could be extracted into ethanol. The extract was run on thin-layer chromatography. An aliquot of ^{3}H-FNLLP was run as marker. (●) Peptide stock. (○) Cell-associated radioactivity.

rate constant of pinocytic uptake is actually twofold greater than previously believed.

Although there is no marked concentration dependence of any of the rate constants studied, detailed examination of the data reveals that k_2 and k_3, the rate constants for further processing and for release respectively, are not entirely independent of the concentration of peptide used. There is a small but consistent decrease in k_3 as well as a small increase in k_2 as the concentration of peptide used goes from 2×10^{-5} M (where 99% of the uptake is via bulk fluid-phase) down to 2×10^{-8} M (80% of the uptake is receptor mediated). Thus there may be a subtle effect of the interaction between receptor and ligand resulting in slightly more release of content taken up by a bulk-fluid-phase than by a receptor-mediated process.

A similar analysis of the release of TCA-precipitable BSA (see Fig. 4) gives a $t_{1/2}$ of release of TCA-precipitable BSA of 3.8 min or a rate constant 0.182 min^{-1}. From studies on the release of BSA we derived values for k_1, k_2, and k_3 (Table I). The values for k_2 and k_3 for fluid-phase uptake of peptide are not significantly different than those for uptake of BSA. However, there is a difference in the values obtained for k_1, the rate constant of endocytosis. The value of k_1 for BSA is approximately an order of magnitude lower than that obtained for

TABLE I

Kinetics of Pinosome Movement

Peptide concentration	U	Rate constant for depletion of Ap*	Total intact peptide released $(Ar_T)^{\ddagger}$	k_1	k_2	k_3	$k_3/k_2 + k_3$	Percent of total uptake which is receptor-mediated
(*M/L*)	(*cpm/cell/min*)	(min^{-1})	(*cpm/cell*)	(*L/cell/min*)	(min^{-1})	(min^{-1})		(min^{-1})
2×10^{-5}	2.5×10^{-3}	0.198	1.3×10^{-2}	4×10^{-14}	0.097	0.101	0.51	<1
2×10^{-6}	2.8×10^{-4}	0.198	1.3×10^{-3}	2.5×10^{-14}	0.095	0.095	0.50	5
2×10^{-7}	7×10^{-5}	0.198	2.4×10^{-4}	5.3×10^{-14}	0.117	0.081	0.41	40
2×10^{-8}	2.5×10^{-5}	0.198	6.2×10^{-5}	1.7×10^{-13}	0.131	0.067	0.34	80
2×10^{-9}	5.5×10^{-6}	0.198	1.5×10^{-5}	1.1×10^{-13}	0.128	0.070	0.35	>90
BSA concentration (cpm/L)								
1.5×10^{10}	9.3×10^{-6}	0.182	6.4×10^{-5}	1.4×10^{-15}	0.080	0.103	0.56	
3.7×10^{9}	4.5×10^{-6}	0.182	3.5×10^{-5}	2.9×10^{-15}	0.076	0.108	0.59	

* This rate constant was measured after uptake in 2×10^{-8} M ^{3}H-FNLLP. We assume that it remains constant after uptake in different concentrations of FNLLP.
‡ Ar_T is the amount of intact peptide (or TCA-precipitable BSA) released in 30 min where the specific activity of ^{3}H-FNLLP is 12.5 Ci/mmol.

bulk-fluid-phase uptake of peptide. Rates of uptake obtained for two other bulk-fluid-phase markers, [^{3}H]sucrose and FITC-dextran were similar to that for BSA (data not shown). Thus there appears to be a low affinity, nonsaturable binding of peptide to the cell surface which results in a rate of peptide uptake slightly greater that a true fluid-phase marker.

DISCUSSION

We have previously shown (7, 35) that chemotactic peptide taken up by PMNs has three possible fates. Some peptide is rapidly released into the medium as intact peptide ($t_{1/2}$ = 3.5 min), some is released more slowly as digested peptide ($t_{1/2}$ = 23 min), and the remainder is stored in the cell for at least 6 h. We now believe we can identify three fates for pinosomes using morphological criteria. Pinosomes can fuse with the plasma membrane with a time course similar to that the release of intact peptide. Pinosomes can also fuse with both the peroxidase-positive and peroxidase-negative electron-dense granules of the PMN. The azurophil granule of the PMN contains myeloperoxidase as well as many lysosomal enzymes and is capable of digesting the peptide. The specific granule contains no proteases and may be the compartment where the storage of peptide occurs.

The release of pinocytosed material in an intact form has been reported for macrophages, hepatocytes, and CHO cells (2, 5, 30, 31). In all three cases, the release was shown to have a $t_{1/2}$ of ~5 min. We examined the uptake of FNLLP and BSA under conditions where uptake is primarily via bulk-fluid-phase and the uptake of FNLLP under conditions where uptake is primarily receptor-mediated. The half-life of release of intact material in both cases is ~4 min.

The termination of the release of intact peptide cannot be explained by the depletion of peptide in the cell since TLC examination of cell-associated radioactivity demonstrate a pool of intact peptide remaining long after the release of intact peptide is complete. Nor can the termination be explained by depletion of pinosomes near the plasma membrane and accumulation in the central regions of the cell where they might be less likely to encounter the plasma membrane. In the presence of metabolic inhibitors and hypertonic sucrose, pinosomes are distributed throughout the cell and yet virtually all of them undergo reverse pinocytosis.

It is possible that there are two parallel pathways of pinocytic uptake: one pathway where pinosomes only fuse with intracellular compartments and a second where pinosomes only fuse with the plasma membrane. We think this possibility unlikely and have both morphological and biochemical data supporting the existence of a single pathway of pinocytic uptake. According to the two compartment hypothesis, uptake in HBSS would be mediated by both classes of pinosomes while in metabolic inhibitors and hypertonic sucrose uptake would only be via a population of pinosomes which rapidly fuse with the plasma membrane. However, the initial rate of ^{3}H-FNLLP uptake and the initial size or distribution of colloidal gold containing vesicles are similar whether uptake is in HBSS or in the inhibitor cocktail. In addition, we have data that a "reversible pinosome" can contribute peptide to the digestion pool. We allowed the reversible pinosome pool to fill with ^{3}H-FNLLP in the presence of the inhibitor cocktail, removed the inhibitors and followed the release of intact and digested peptide during further incubation in HBSS at 37°C. If there are two pathways of uptake, then all the pinosomes formed in the presence of the inhibitor cocktail will only be able to fuse with the plasma membrane and none will fuse with the digestion compartment even when the inhibitor block has been removed. However, there is significantly more digested peptide released from these cells than from cells maintained in the inhibitor cocktail (unpublished results). Thus we believe that there is a single pathway of pinocytic uptake and that the same compartment which can undergo reverse pinocytosis can also deliver material to the digestion (and storage) pools.

The mechanism by which approximately half of the fluid internalized is rapidly returned to the medium is unclear. It could be that the newly formed pinosomes have a certain probability of fusing with the plasma membrane before they are modified or fuse with some internal compartment. Alternatively, all the pinosomes might first fuse with an internal compartment from which vesicles would carry part of the content of this compartment to the outside and part to other internal compartments. We have defined the reversible pinocytic compartment as the source of released intact material, but we cannot say whether the content of this compartment is identical in composition to the material initially internalized or whether it has been altered prior to its exocytosis. Whatever modification may be occurring in the pinocytic compartment in PMNs, it is clear from the differential effects of the inhibitor cocktail that there is separate control over the fusion of the pinosome with the plasma membrane and its fusion with the

cytoplasmic granules. We do not believe that the reversible pinocytosis is energy-independent but merely that it is less energy-dependent than other fates of the pinosome. This is consistent with the observations by Dunn et al. (8) that low temperature (≤15°C) reversibility inhibits the accumulation of asialoglycoproteins in the lysosomes of liver cells but does not inhibit their uptake.

Clearly there are multiple levels of complexity in the postendocytic compartmentation of pinocytic markers. Both receptor-ligand interactions as well as the regulation of the fusion between pinosomes and various subcellular compartments appear to be important (6, 21). The biochemical and morphological description of pinocytosis in PMNs is now a well characterized system in which to examine factors which control the fusion of pinosomes with the different granules and with the plasma membrane.

APPENDIX

The movement of pinocytosed material is characterized by three processes: (*a*) the rate of uptake of material into pinosomes is proportional to M_o, the concentration of extracellular peptide, with endocytosis rate constant k_1; (*b*) the rate of release of intact material is proportional to A_p, the amount of peptide in the reversible pinocytic pool, with release rate constant k_3; and (*c*) the rate of movement of material into the digestion and storage pools is also proportional to A_p, with rate constant k_2. Given these assumptions, the rate of filling of the pinocytic pool during incubation in extracellular peptide is

$$\frac{dA_p}{dt} = k_1M_o - (k_2 + k_3)A_p, \tag{1}$$

during the time period $0 < t < t'$, where t' is the incubation time. The rate of emptying of the reversible pool after the extracellular peptide is removed is

$$\frac{dA_p}{dt} = -(k_2 + k_3)A_p, \tag{2}$$

during the time period $t' < t < T$, where $(T - t')$ is the duration of the release experiment. The rate of accumulation of released material in the extracellular medium during this time period is

$$\frac{dA_r}{dt} = k_3A_p. \tag{3}$$

Eq. 1 can be integrated over t from 0 to t', to obtain the amount of peptide in the reversible pool at t':

$$A_p(t') = \frac{k_1M_o}{k_2 + k_3}[1 - e^{-(k_2+k_3)t'}]. \tag{4}$$

Eq. 2 can be integrated over t from t' to get

$$A_p(t) = A_p(t')e^{-(k_2+k_3)(t-t')}. \tag{5}$$

We can then substitute Eq. 5 into Eq. 3, and by integrating over t from t' obtain the amount released after incubation:

$$A_r(t) - A_r(t') = \frac{k_3k_1M_o}{(k_2+k_3)^2}[1 - e^{-(k_2+k_3)t'}] \cdot[1 - e^{-(k_2+k_3)(t-t')}]. \tag{6}$$

For long incubation times (i.e., $t \gg (k_2 + k_3)^{-1}$), the amount released after incubation will reach a plateau, which is

$$A_{r\infty} = \frac{k_3k_1M_o}{(k_2 + k_3)^2}. \tag{7}$$

Then a plot of

$$\ln\left\{1 - \frac{A_r(t) - A_r(t')}{A_{r\infty}}\right\} \text{ vs. } (t - t')$$

or ln of percent peptide remaining in cell as a function of release time (see Fig. 9 *b*) should yield a straight line with

$$\text{slope} = -(k_2 + k_3). \tag{8}$$

Now, the total peptide uptake rate is equal to U, where

$$U = k_1M_o - k_3A_p. \tag{9}$$

When the pinocytic pool is at steady state, containing amount A_{pss}, then

$$k_1M_o - k_3A_{pss} = k_2A_{pss}. \tag{10}$$

Therefore, the peptide uptake rate at steady state, U_{ss}, is

$$U_{ss} = k_2A_{pss} = \frac{k_1k_2M_o}{K_2 + k_3}. \tag{11}$$

We now can determine values for the rate constants k_1, k_2, k_3 from Eqs. 7, 8, and 11.
Defining $c_1 = k_2 + k_3$, from Eq. 8, $c_2 = k_1k_3$, from Eq. 7, and $c_3 = k_1k_2$, from Eq. 11, we obtain $k_1 = (c_2 + c_3)/c_1$, $k_2 = c_1c_3/(c_2 + c_3)$, and $k_3 = c_1c_2/(c_2 + c_3)$.

The authors thank Joan Slonczewski and Susan Sullivan for reading the manuscript and offering helpful suggestions, Amy Woodworth for excellent technical assistance, and Betti Goren and John Woolsey for the art work.

The work was supported by National Science Foundation grant PCM-80-18585 to S. H. Zigmond.

Received for publication 8 October 1982, and in revised form 25 February 1983.

REFERENCES

1. Abrahamson, D. R., and R. Rodewald. 1981. Evidence of the sorting of endocytic vesicle contents during receptor-mediated transport of IgG across the new born rat intestine. *J. Cell Biol.* 91:270–280.
2. Adams, C. J., K. M. Maurey, and B. Storrie. 1982. Exocytosis of pinocytic contents by Chinese hamster ovary cells. *J. Cell Biol.* 93:632–637.
3. Anderson, R. G. W., M. S. Brown, U. Beisiegel, and J. L. Goldstein. Surface distribution and recycling of the LDL receptor as visualized with antireceptor antibodies. *J. Cell Biol.* 93:523–531.
4. Bainton, D. F., and M. G. Farquhar. 1968. Differences in enzyme content of azurophil and specific granules in polymorphonuclear leukocytes. *J. Cell Biol.* 39:299–317.
5. Besterman, J. M., J. A. Airhart, R. C. Woodworth, and B. Low. 1981. Exocytosis of pinocytosed fluid in cultured cells: kinetic evidence for rapid turnover and compartmentalization. *J. Cell Biol.* 91:716–727.
6. Connolly, D. T., R. R. Townsend, K. Kawaguchi, W. R. Bell, and Y. C. Lee. 1982. Binding and endocytosis of cluster glycosides by rabbit hepatocytes. *J. Biol. Chem.* 257:939–945.
7. Daukas, G., P. Kuwabra, B. Binczewski, S. Sullivan, and S. Zigmond. 1981. Reversible pinocytosis in PMNs. *J. Cell Biol.* 91(2, Pt. 2):412*a*. (Abstr.)
8. Dunn, W. A., A. C. Hubbard, and N. N. Aronson. 1980. Low temperature selectively inhibits fusion between pinocytic vesicles and lysosomes during heterophagy of ^{125}I-asialofetuin by the perfused rat liver. *J. Biol. Chem.* 255:5971–5978.
9. Deleted in proof.
10. Ehrenreich, B. A., and Z. A. Cohn. 1969. The fate of peptides pinocytosed by macrophages in vitro. *J. Exp. Med.* 129:227–243.
11. Farquhar, M. G. 1978. Recovery of surface membrane in anterior pituitary cells. Variations in traffic detected with anionic and catonic ferritin. *J. Cell. Biol.* 77:R35–R42.
12. Geoghegan, W. D., and G. A. Ackerman. 1977. Adsorption of horseradish peroxidase, ovomucoid and anti-immunoglobin to colloidal gold for indirect detection of concanavalin A, wheat germ agglutinin and goat antihuman immunoglobin G on cell surfaces at the electron microscopic level: a new method, theory and application. *J. Histochem. Cytochem.* 25:1187–1200.
13. Graham, R. C., and M. J. Karnovsky. 1966. The early stages of absorption of injected horseradish peroxidase in the proximal tubules of mouse kidney: ultrastructural cytochemistry by a new technique. *J. Histochem. Cytochem.* 14:291–302.

14. Henson, J. E., and P. E. Henson. 1981. Neutrophil secretion with alterations in granule morphology (dissolution) and formation of coated vesicles. *J. Cell Biol.* 91(2, Pt. 2):242*a*. (Abstr.)
15. Horisberger, M., and J. Rosset. 1977. Colloidal gold, a useful marker for transmission and scanning electron microscopy. *J. Histochem Cytochem.* 25:295–305.
16. Hunter, W. M., and F. C. Greenwood. 1962. Preparation of iodine-131 labelled human growth hormone of high specific activity. *Nature (Lond.).* 194:495–496.
17. Deleted in proof.
18. Lloyd, J. B. 1971. A study of permeability of lysosomes to amino acids and small peptides. *Biochem. J.* 121:245–248.
19. Muller, W. A., R. M. Steinman, and Z. A. Cohn. 1980. The membrane proteins of the vacuolar system. II. Bidirectional flow between secondary lysosomes and plasma membrane. *J. Cell Biol.* 86:304–314.
20. Niedel, J., I. Kalane, and P. Cuatrecasas. 1979. Receptor-mediated internalization of fluorescent chemotactic peptide by human neutrophils. *J. Biol. Chem.* 254:10700–10706.
21. Opresko, L., H. S. Wiley, and R. A. Wallace. 1980. Differential postendocytotic compartmentation in Xenopus oocytes is mediated by a specifically bound ligand. *Cell.* 22:47–57.
22. Pastan, I., and M. C. Willingham. 1981. Receptor-mediated endocytosis of hormones in cultured cells. *Annu. Rev. Physiol.* 43:239–250.
23. Peachey, L. D. 1971. A simple device for rapid morphometric analysis using a small digital computer. *Proceedings of the Royal Microscopy Society.* 6:214. (Abstr.)
24. Peachey, L. D. 1981. A relatively inexpensive microprocessor-linked digital planimeter for electron microscopic morphometry. 39th Annual Proceedings of the Electron Microscopy Society of America. G. W. Bailey, editor. Atlanta, GA. 266–269.
25. Schneider, Y. J., P. Tulkens, C. de Duve, and S. Trouet. 1979. Fate of plasma membrane during endocytosis. II. Evidence for recycling (shuttle) of plasma membrane components. *J. Cell Biol.* 82:466–478.
26. Deleted in proof.
27. Spurr, A. R. 1969. A low-viscosity epoxy resin embedding medium for electron microscopy. *J. Ultrastruct. Res.* 26:31–42.
28. Steinman, R. M., S. E. Brodie, and Z. A. Cohn. 1976. Membrane flow during pinocytosis: a stereologic analysis. *J. Cell Biol.* 68:665–687.
29. Sullivan, S. J., and S. H. Zigmond. 1980. Chemotactic peptide receptor modulation in polymorphonuclear leukocytes. *J. Cell Biol.* 85:703–711.
30. Tietze, C., P. Schlesinger, and P. Stahl. 1982. Mannose-specific endocytosis receptor of alveolar macrophages: demonstration of two functionally distinct intracellular pools of receptor and their roles in receptor recycling. *J. Cell Biol.* 92:417–424.
31. Tolleshaug, H., P. A. Chindemi, and E. Regoeczi. 1981. Diacytosis of human asialotransferrin type 3 by isolated rat hepatocytes. *J. Biol. Chem.* 256:6526–6528.
32. Wall, D. A., G. Wilson, and A. L. Hubbard. 1980. The galactose-specific recognition system of mammalian liver: the route of ligand internalization in rat hepatocytes. *Cell.* 21:79–93.
33. Widnell, E. E.,Y. J. Schneider, B. Pierre, P. Baudhuin, and A. Trouet. 1982. Evidence for a continued exchange of 5′-nucleotidase between the cell surface and cytoplasmic membranes in cultured rat fibroblasts. *Cell.* 28:61–70.
34. Deleted in proof.
35. Zigmond, S. H., S. J. Sullivan, and D. A. Lauffenburger. 1982. Kinetic analysis of chemotactic peptide receptor modulation. *J. Cell Biol.* 92:34–43.